

# Levels in $^{189}\text{Ir}$ and $^{191}\text{Ir}$ observed in the $(p, t)$ reaction

Gordon L. Struble, Robert G. Lanier, and Lloyd G. Mann

*University of California, Lawrence Livermore Laboratory, Livermore, California 94550*

Raymond K. Sheline

*Florida State University, Tallahassee, Florida 32306*

Richard T. Kouzes, William H. Moore, Dennis Mueller, Robert A. Naumann, and Ivan C. Oelrich†

*Princeton University, Princeton, New Jersey 08540*

(Received 6 December 1977)

Levels in  $^{189}\text{Ir}$  and  $^{191}\text{Ir}$  were populated by the  $(p, t)$  reaction, using 34-MeV protons and isotopically enriched  $^{191}\text{Ir}$  and  $^{193}\text{Ir}$  targets. A number of low-lying positive-parity bands were observed. In addition the  $11/2^- [505]$  bandhead was also weakly populated. The  $3/2^- 1/2^+ [400]$  states in  $^{189}\text{Ir}$  and  $^{191}\text{Ir}$  have similar but anomalous angular distributions. Four strongly populated states with  $L = 0$  angular distributions are observed from 719 to 1261 keV in  $^{189}\text{Ir}$ . For the same energy region in  $^{191}\text{Ir}$ , the  $L = 0$  states are less strongly populated.

[NUCLEAR REACTIONS  $^{191}\text{Ir}(p, t)$  and  $^{193}\text{Ir}(p, t)$ ,  $E_{\text{lab}} = 34.7$  MeV; measured  $\sigma(\theta)$ ; deduced  $E_x, L, J^\pi$  of  $^{189}\text{Ir}$  and  $^{191}\text{Ir}$  levels.]

## I. INTRODUCTION

The Ir isotopes lie in an interesting position between the rare earth nuclei, which exhibit permanent prolate deformation, and the  $^{208}\text{Pb}$  nucleus, which has a doubly closed shell. Indeed a sudden change in the ground-state deformation between  $Z = 76$  and  $Z = 78$  has been predicted,<sup>1,2</sup> and the measured quadrupole moments for the first excited states of the even-even nuclei have different signs.<sup>3</sup> In the intermediate odd-proton Ir isotopes, the odd proton can serve as a probe of a variety of possible collective shapes of the core. Among the different possible core configurations, which might exist alone or coexist in  $^{189}\text{Ir}$  and  $^{191}\text{Ir}$ , are simple prolate, oblate, triaxial, and  $\gamma$ -unstable shapes.

The nuclei  $^{189}\text{Ir}$  and  $^{191}\text{Ir}$  have been investigated thoroughly following the radioactive decay of, respectively,  $^{189}\text{Pt}$  (Hedin and Backlin<sup>4</sup>) and  $^{191}\text{Pt}$  (Price and Johns<sup>5</sup>). The  $(^3\text{He}, d)$  and  $(d, d')$  reactions<sup>6,7</sup> have also been valuable in identifying intrinsic and collective configurations for  $^{191}\text{Ir}$ . These studies suggested the existence of a number of rotational bands built on prolate Nilsson states, although triaxial shapes were not ruled out. The states include those built on the  $\frac{3}{2}^+ [402]$ ,  $\frac{1}{2}^+ [400]$ ,  $\frac{1}{2}^- [505]$ , and, in the case of  $^{191}\text{Ir}$ , the  $\frac{1}{2}^+ [411]$  Nilsson configurations. Recent  $(\alpha, xn\gamma)$  and  $(p, n\gamma)$  studies<sup>8,9</sup> of  $^{189}\text{Ir}$  disclosed rotational bands built on the intrinsic Nilsson states to high spin and in addition have shown the existence of the  $\frac{3}{2}^- [514]$  rotational band. It has also been suggested<sup>8</sup> that Nilsson states for the positive-parity bands may

coexist with rotational aligned and triaxial negative-parity bands.

The goal of the present  $(p, t)$  experiment is to relate states in the residual nuclei to the ground-state configurations in the target nuclei. For superfluid nuclei, almost all the two-neutron transfer strength populates states of the product nucleus that are closely related to the ground state of the target nucleus. If the target nucleus and the residual nucleus have the same shape and if there is no appreciable Coriolis coupling, then almost all the two-nucleon strength should appear in the ground-state rotational band. Thus, the  $(p, t)$  reaction is a sensitive probe for deviations from the simple strong-coupling model, and it is of particular interest for understanding nuclei in regions where shape transitions occur. A comparison of  $^{193}\text{Ir}(p, t)$ ,  $^{191}\text{Ir}(p, t)$ , and  $^{189}\text{Ir}(p, t)$  reactions is especially interesting since the measured electromagnetic transition probabilities<sup>4</sup> suggest a change in nuclear deformation between  $^{191}\text{Ir}$  and  $^{189}\text{Ir}$  possibly as large as a factor of two.

In Sec. II we describe the experimental procedure. The results of the experiments are presented in Sec. III. Section IV contains a discussion and interpretation of the results, while Sec. V is a brief summary and conclusion.

## II. EXPERIMENTAL PROCEDURE

Targets of  $^{191}\text{Ir}$  and  $^{193}\text{Ir}$ , 56 and 40  $\mu\text{g}/\text{cm}^2$  thick, respectively, were prepared at Florida State University by slow (8–12 h per target) evaporation of the iridium metal onto a 44- $\mu\text{g}/\text{cm}^2$  carbon foil

using electron bombardment. Target thicknesses were measured with a Sloan thickness gauge and are believed accurate to  $\pm 25\%$ . The  $^{191}\text{Ir}$  and  $^{193}\text{Ir}$  isotopes, which were obtained from the Stable Isotopes Division of the Oak Ridge National Laboratory, were enriched to 94.66% and 98.70%, respectively.

A 34.7-MeV proton beam from the Princeton AVF cyclotron was used to produce the  $^{191,193}\text{Ir}(p,t)$   $^{189,191}\text{Ir}$  reactions. Spectra were recorded at angles from  $15^\circ$  to  $60^\circ$  in  $5^\circ$  steps. Tritons were momentum-analyzed by a quadrupole-dipole-dipole-dipole magnetic spectrograph and detected by a 60-cm position-sensitive wire proportional counter backed with a plastic scintillator. The detector spanned an excitation energy range from the ground state to approximately 1.5 MeV. A resolution of 13 keV full width at half maximum (FWHM) was achieved using a spectrograph solid angle of 11.8 msr.

Excitation energies in both nuclei were determined by calibration of the spectrograph focal plane using previously known energies of levels in  $^{189}\text{Ir}$ . Energies were determined using peak positions from spectra taken at  $10^\circ$  and  $25^\circ$ ; the two determinations of energy values agree within 2 keV.

The positions and areas of the peaks were deter-

mined at each angle using the spectrum-analysis computer code AUTOFIT. Only peaks which were statistically significant at all of the angles were accepted as peaks attributed to Ir nuclei. Unfortunately we were unable to normalize our experiments at different angles by use of a monitor detector. Therefore, in order to quote cross sections we carefully measured the integrated current at each angle and used an independent measure of the target thickness to calculate the differential cross section. Although the targets were very uniform, we believe that this procedure may have introduced systematic errors as large as 25% in the absolute cross sections. However, the relative cross sections at a given angle should be within the statistical error, and the relative cross sections at different angles should have no more than a 4% systematic error.

### III. RESULTS

Figures 1 and 2 display triton spectra taken at  $10^\circ$  with respect to the beam for  $^{189}\text{Ir}$  and  $^{191}\text{Ir}$ , respectively. In Table I we present the excitation energies and intensities of levels in  $^{189}\text{Ir}$  and  $^{191}\text{Ir}$  observed in the  $(p,t)$  reaction. These energies and intensities were determined using the techni-

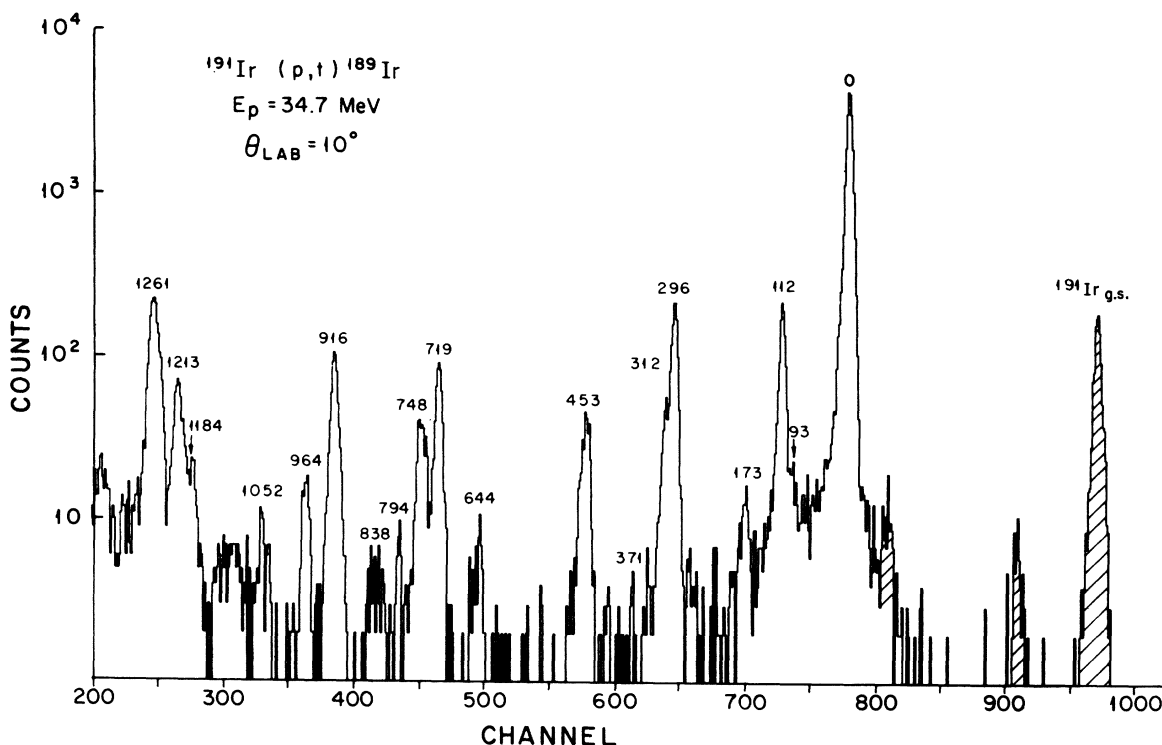


FIG. 1. The triton spectrum from the reaction  $^{191}\text{Ir}(p,t)^{189}\text{Ir}$ . The levels in  $^{189}\text{Ir}$  are labeled with the excitation energy in keV.

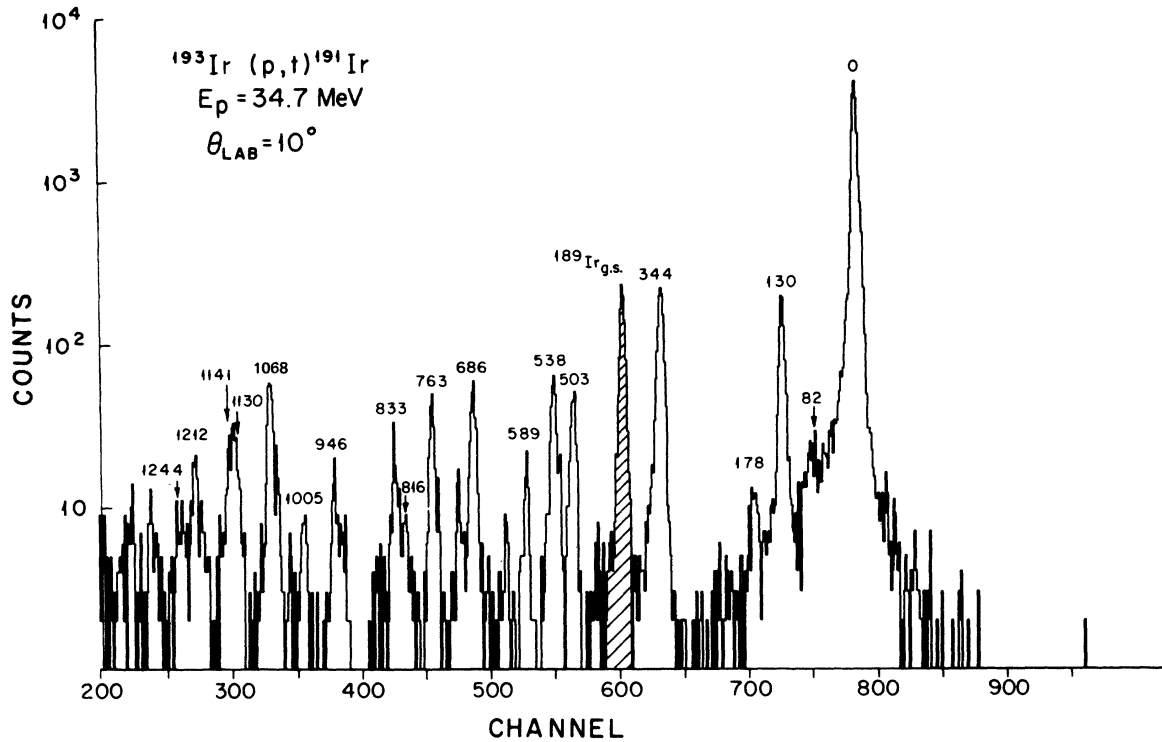


FIG. 2. The triton spectrum from the reaction  $^{193}\text{Ir}(p,t)^{191}\text{Ir}$ . The levels in  $^{191}\text{Ir}$  are labeled with the excitation energy in keV.

TABLE I. Energies and summed cross sections ( $\Sigma d\sigma/d\Omega \sin\theta$ ) for the  $^{191}\text{Ir}(p,t)^{189}\text{Ir}$  and  $^{193}\text{Ir}(p,t)^{191}\text{Ir}$  reactions.

$^{189}\text{Ir}$			$^{191}\text{Ir}$		
Energy (keV)	Cross section ( $\mu\text{b}$ )	$L$	Energy (keV)	Cross section ( $\mu\text{b}$ )	$L$
0	243.8	0	0	242.5	0
93	2.2		82	2.6	
112	15.8		130	15.5	
173	1.4		178	1.8	
296	16.6		344	20.5	
312	3.1		503	4.6	
371	0.2		538	4.8	0
453	3.9		589	1.3	
644	0.3		686	4.3	
719	6.2	0	763	2.5	0
748	3.4		816	1.4	
794	0.3		833	2.6	
838	0.4		946	1.4	
916	8.0	0	1005	2.0	
964	1.2		1068	4.0	0
1052	0.3	0	1130	2.8	
1184	3.4		1141	4.1	
1213	5.4	0	1212	2.0	
1261	19.1	0	1244	1.3	

ques discussed in Sec. II. In the subsequent interpretation of the data, we observed evidence for additional peaks. We quote these energies in Sec. IV (see Figs. 9 and 10); however, these peaks are so tentative that we do not include them in Table I. The intensities quoted in Table I are obtained by summing the differential cross sections weighted by the sine of their respective laboratory angles.

The angular distributions of the levels quoted in Table I are presented in Figs. 3–5 for  $^{189}\text{Ir}$  and Figs. 6–8 for  $^{191}\text{Ir}$ . The differential cross sections are plotted in arbitrary units. To obtain differential cross sections in units of  $\mu\text{b}/\text{sr}$ , one must multiply by factors of 0.074 and 0.10 for  $^{189}\text{Ir}$  and  $^{191}\text{Ir}$ , respectively. The  $L=0$  transitions for 35-MeV protons<sup>10</sup> are easily identified. If we assume the ground-state spins and parities of the target nuclides are  $\frac{3}{2}^+$  (see discussion in Sec. IV), such distributions uniquely define the spin and parity of a level as  $\frac{3}{2}^+$ . Levels that have been identified as  $\frac{3}{2}^+$  from the analysis in Sec. IV are displayed in Figs. 3 and 6. The angular distributions of those levels whose spins and parities allow an  $L=2$  component are presented in Figs. 4 and 7.

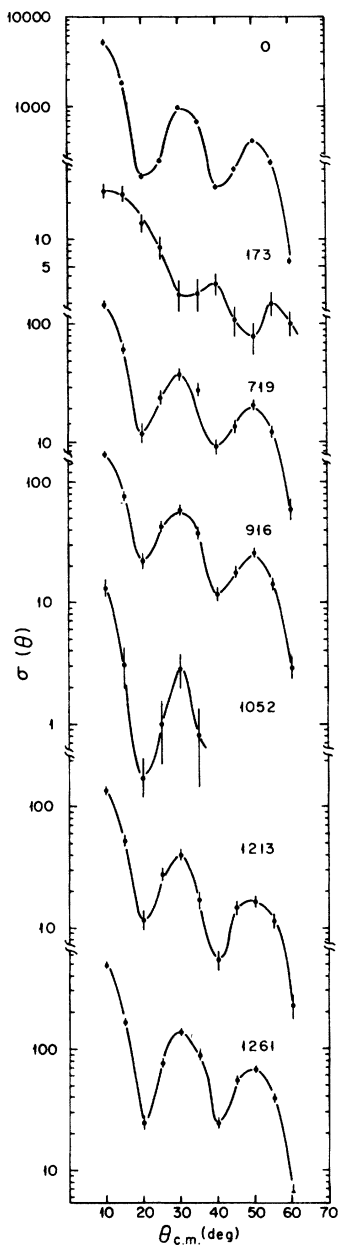


FIG. 3. Angular distributions of states concerning  $L = 0$  transitions from the reaction  $^{191}\text{Ir}(p, t)^{189}\text{Ir}$ . The differential cross sections are plotted using an arbitrary scale and must be multiplied by a factor of 0.074 to convert to units of  $\mu\text{b}/\text{sr}$ .

The distributions for the remaining levels are plotted in Figs. 5 and 8. These figures are discussed in more detail in the next section.

#### IV. DISCUSSION

The  $(p, t)$  reaction tends to select those states in the residual nuclei which are closely related to the

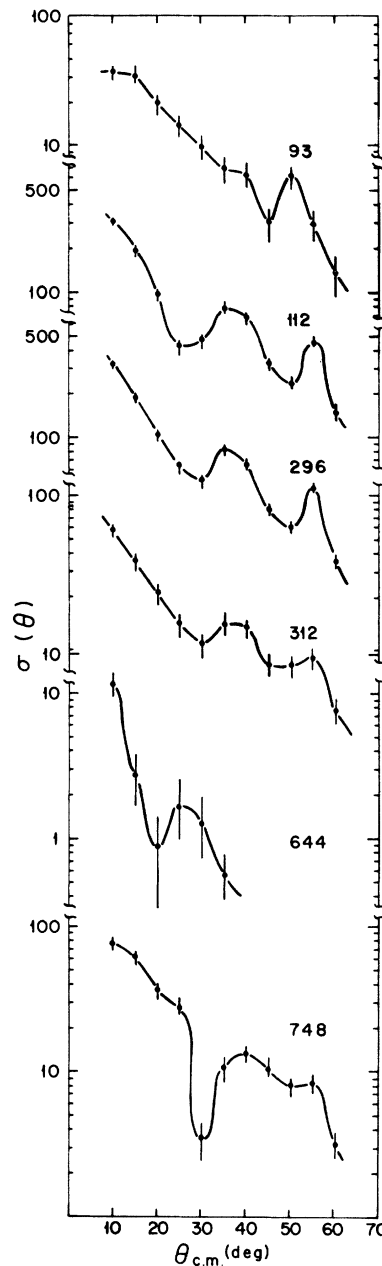


FIG. 4. Angular distributions of states consistent with  $L = 2$  transitions from the reaction  $^{191}\text{Ir}(p, t)^{189}\text{Ir}$ . The differential cross sections are plotted using an arbitrary scale and must be multiplied by a factor of 0.074 to convert to units of  $\mu\text{b}/\text{sr}$ .

ground states of the target nuclei. It is therefore of value to discuss the nature of the ground state in the target nuclei  $^{191}\text{Ir}$  and  $^{193}\text{Ir}$ . Decay scheme studies<sup>5,11</sup> and studies of proton stripping reactions<sup>6</sup> indicate that the ground states of both these nuclei can best be described as the  $\frac{3}{2}^+$  bandhead of the proton Nilsson orbital  $\frac{3}{2}^+ [402\frac{1}{2}]$ . The  $C_{ji}^2 U^2$  factors

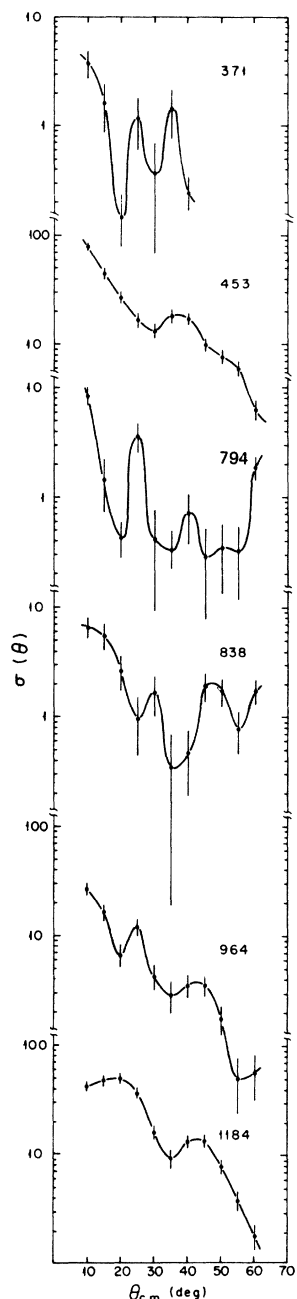


FIG. 5. Angular distributions of states not consistent with either  $L=0$  or  $L=2$  transitions from the reaction  $^{191}\text{Ir}(p,t)^{189}\text{Ir}$ . The differential cross sections are plotted using an arbitrary scale and must be multiplied by a factor of 0.074 to convert to units of  $\mu\text{b}/\text{sr}$ .

deduced from the charged-particle spectra<sup>6</sup> leave little doubt about this assignment. Thus we would expect that the predominant features of the  $(p,t)$  spectra will be the  $\frac{3}{2}^+[402]$  bands in  $^{189}\text{Ir}$  and  $^{191}\text{Ir}$ , together with any positive-parity states with which these bands are coupled through Coriolis or vibra-

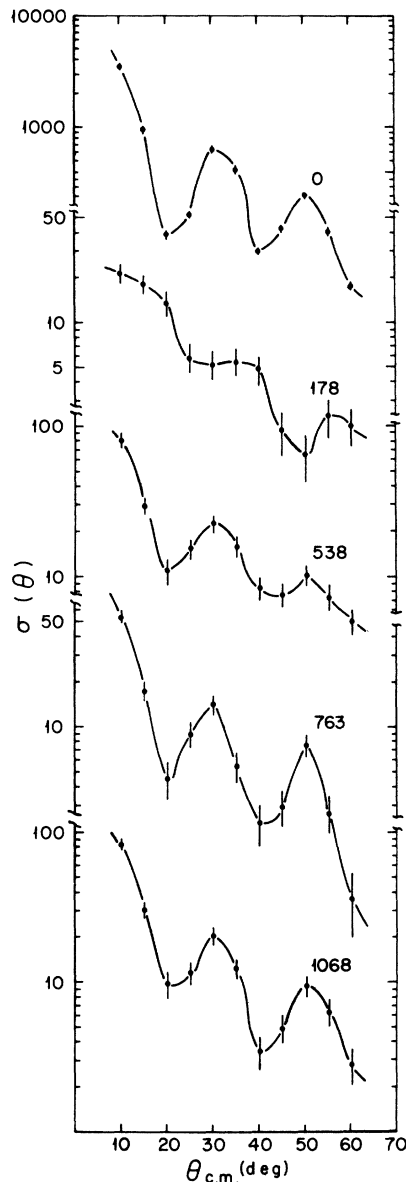


FIG. 6. Angular distributions of states containing  $L=0$  transitions from the reaction  $^{193}\text{Ir}(p,t)^{191}\text{Ir}$ . The differential cross sections are plotted using an arbitrary scale and must be multiplied by a factor of 0.10 to convert to units of  $\mu\text{b}/\text{sr}$ .

tion-particle interactions. Figures 9 and 10 present our interpretation of the  $(p,t)$  data in terms of the Nilsson model.

#### A. $\frac{3}{2}^+[402\frac{1}{2}]$ orbital

The  $\frac{3}{2}^+[402\frac{1}{2}]$  orbital has previously been demonstrated conclusively to be the ground-state rotational band for both  $^{189}\text{Ir}$  and  $^{191}\text{Ir}$ . In the case of  $^{189}\text{Ir}$  the band was earlier<sup>4</sup> identified up to the  $\frac{7}{2}^+$  mem-

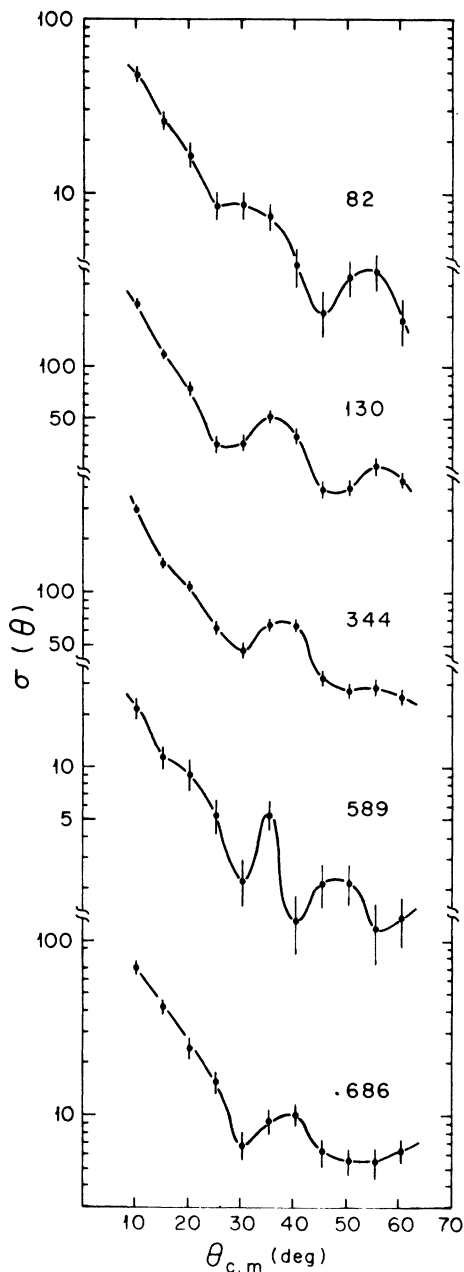


FIG. 7. Angular distributions of states consistent with  $L=2$  transitions from the reaction  $^{189}\text{Ir}(p, t)^{191}\text{Ir}$ . The differential cross sections are plotted using an arbitrary scale and must be multiplied by a factor of 0.10 to convert to units of  $\mu\text{b/sr}$ .

ber and later<sup>8,9</sup> up to the  $\frac{7}{2}^+$  member. In the case of  $^{191}\text{Ir}$  there is convincing evidence for the Nilsson assignment<sup>6</sup> up to spin  $\frac{7}{2}^+$ . Since the ground states of the target nuclei are also  $\frac{3}{2}^+$  [402+] it is not surprising that the most prominent features of  $(p, t)$  spectra are the  $\frac{3}{2}^+$  [402+] ground-state bands in both  $^{189}\text{Ir}$  and  $^{191}\text{Ir}$ . They are clearly observed

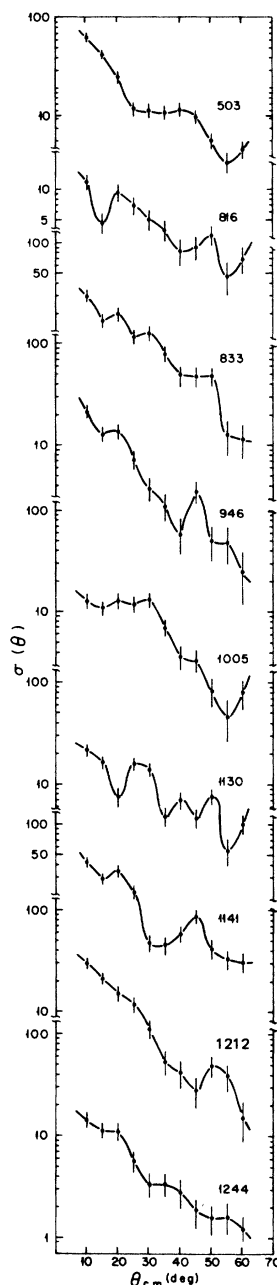


FIG. 8. Angular distributions of states not consistent with either  $L=0$  or  $L=2$  transitions from the reaction  $^{189}\text{Ir}(p, t)^{191}\text{Ir}$ . The differential cross sections are plotted using an arbitrary scale and must be multiplied by a factor of 0.10 to convert to units of  $\mu\text{b/sr}$ .

up to the  $\frac{7}{2}^+$  members in each nucleus with generally decreasing intensity as the spin increases but with the  $\frac{7}{2}^+$  member somewhat more strongly populated than the general trend. The state at 833 keV has approximately the right energy and intensity to be the  $\frac{7}{2}^+$  member of the  $^{191}\text{Ir}$  ground-state band. However, the evidence is too weak to make a posi-

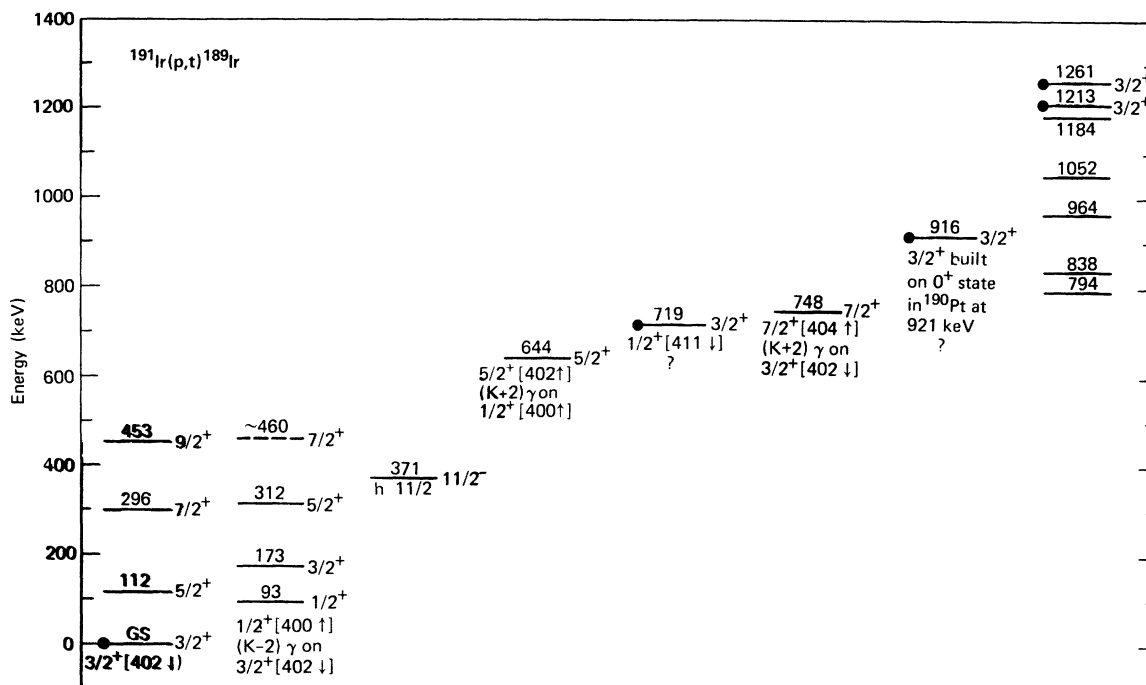


FIG. 9. Levels in  $^{189}\text{Ir}$  populated in the reaction  $^{191}\text{Ir}(p,t)^{189}\text{Ir}$ . Dashed levels represent tentative assignments (see text).  $L=0$  angular distributions are represented with a solid circle to the left of the level.

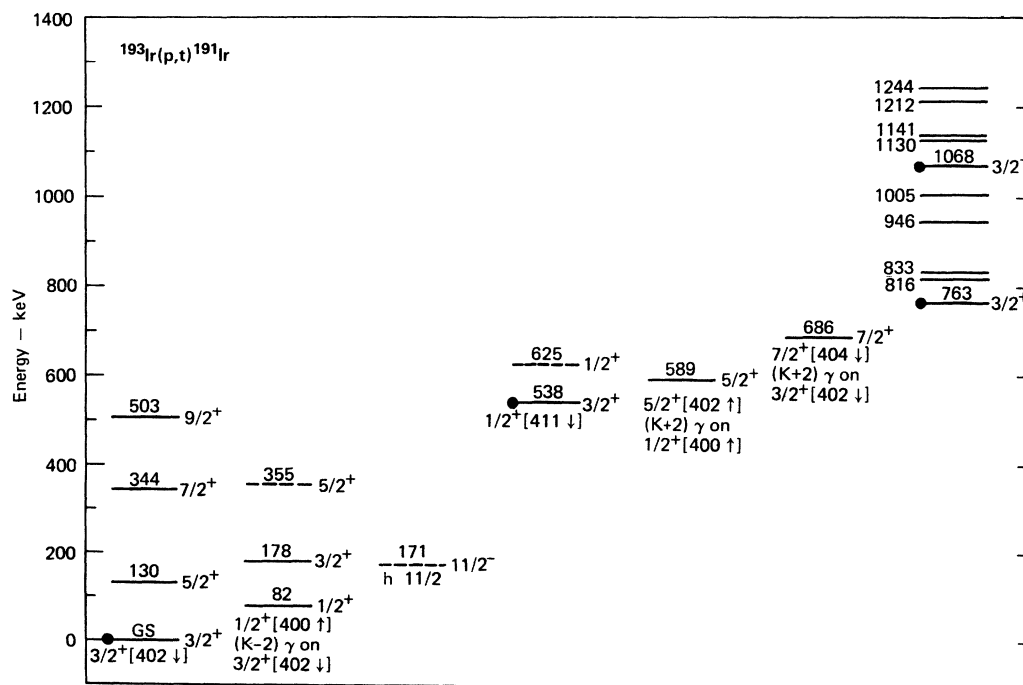


FIG. 10. Levels in  $^{191}\text{Ir}$  populated in the reaction  $^{193}\text{Ir}(p,t)^{191}\text{Ir}$ . Dashed levels represent tentative assignments (see text).  $L=0$  angular distributions are represented with a solid circle to the left of the level.

tive identification. The previously known  $\frac{11}{2}^+$  state in  $^{189}\text{Ir}$  at 745.7 keV is too close to the state at 751 keV for positive identification in our measurements, although structure on the low-energy side of the 751-keV state may suggest this interpretation.

#### B. $\frac{1}{2}^+$ [400 $\uparrow$ ] orbital

In a variety of earlier work<sup>4-9</sup> a state at 94 keV in  $^{189}\text{Ir}$  and one at 82 keV in  $^{191}\text{Ir}$  were attributed to the  $\frac{1}{2}^+$  [400 $\uparrow$ ] bandhead. Rotational members of this band as high as  $\frac{15}{2}^+$  have been observed<sup>9</sup> in  $^{189}\text{Ir}$ , and as high as  $\frac{5}{2}^+$  in  $^{191}\text{Ir}$ .<sup>6</sup> It is of considerable interest that the lowest members of this band in  $^{191}\text{Ir}$  were populated<sup>7</sup> both by inelastic scattering and Coulomb excitation. The  $B(E2)$  values connecting these levels with the  $\frac{3}{2}^+$  [402 $\uparrow$ ] ground state were shown to be approximately six single-particle units, a very large figure. Furthermore, the  $C_{J1}^2 U^2$  values for populating the various members of the  $\frac{1}{2}^+$  [400 $\uparrow$ ] band of  $^{191}\text{Ir}$  by proton stripping were in good relative agreement with theory but only about one-half the expected absolute intensities. Both of these experiments strongly suggest that the  $I = \frac{1}{2}^+$  state at 82 keV in  $^{191}\text{Ir}$  is approximately 50% a single-particle (the  $\frac{1}{2}^+$  [400 $\uparrow$ ] Nilsson state) and 50% a  $(K-2)$   $\gamma$ -phonon state based on the  $\frac{3}{2}^+$  [402 $\uparrow$ ] ground state. This strong admixture is expected since the  $\frac{1}{2}^+$  [400 $\uparrow$ ] and  $\frac{3}{2}^+$  [402 $\uparrow$ ] orbitals satisfy the selection rules for coupling by large  $E2$  matrix elements. We should also note that the  $\frac{1}{2}^+$  [400 $\uparrow$ ] and  $\frac{3}{2}^+$  [402 $\uparrow$ ] orbitals can Coriolis couple with each other. Finally the  $\frac{3}{2}^+$  [402 $\uparrow$ ] ground-state band is expected to contain admixtures of the  $(K-2)$   $\gamma$  band built on the  $\frac{1}{2}^+$  [400 $\uparrow$ ] band. For these reasons (assuming the same mixing occurs in  $^{189}\text{Ir}$ ), we would expect to see considerable population of the  $\frac{1}{2}^+$  [400 $\uparrow$ ] bands in the  $(p, t)$  reactions. In both nuclei we found that this band is populated up to the  $\frac{5}{2}^+$  rotational member, although the intensity is weaker than we anticipated.

#### C. $\frac{1}{2}^-$ [505 $\uparrow$ ] orbital

The  $\frac{11}{2}^-$  [505 $\uparrow$ ] orbital has been observed as an isomeric state at 372 keV<sup>8,9</sup> in  $^{189}\text{Ir}$  and at 171 keV<sup>6</sup> in  $^{191}\text{Ir}$ . A very weak state was observed in our  $(p, t)$  studies in  $^{189}\text{Ir}$  at 371 keV. Although a state at 178 keV interferes with the observation of a weak  $\frac{11}{2}^-$  state at 171 keV in  $^{191}\text{Ir}$ , some indication of structure on the low-energy side of the 178-keV state is evident. Because this  $\frac{11}{2}^-$  state in  $^{189}\text{Ir}$  is the only negative-parity state populated in this study and because of the suggested structures for this state, we postpone further discussion.

#### D. $\frac{1}{2}^+$ [411 $\downarrow$ ] orbital

It has been suggested<sup>6</sup> that the  $\frac{1}{2}^+$  [411 $\downarrow$ ] band in  $^{191}\text{Ir}$ , which is expected to have the  $\frac{1}{2}^+$  and  $\frac{3}{2}^+$  states inverted in energy, has been observed with the  $\frac{3}{2}^+$  state occurring at 539 keV and the  $\frac{1}{2}^+$  state at 624 keV. We observe the  $\frac{3}{2}^+$  state with  $L=0$  angular distribution at 538 keV and observe a very weak state at approximately 625 keV which may be the  $\frac{1}{2}^+$  state. The corresponding  $\frac{3}{2}^+$  state is observed at 719 keV in  $^{189}\text{Ir}$ .

#### E. $\frac{5}{2}^+$ [402 $\uparrow$ ] orbital

A  $\frac{5}{2}^+$  state at 588 keV in  $^{191}\text{Ir}$  has previously been observed in decay scheme studies.<sup>5</sup> This state is populated in proton stripping reactions somewhat more strongly than expected for its assignment as the  $\frac{5}{2}^+$  [402 $\uparrow$ ] bandhead. However, since it is the only  $\frac{5}{2}^+$  state expected in this region we tentatively concur in this identification. It is interesting to note that this state is expected to have some admixture of the  $(K+2)$   $\gamma$  band built on the  $\frac{1}{2}^+$  [400 $\uparrow$ ] orbital. This state is populated in the  $(p, t)$  reaction at 589 keV in  $^{191}\text{Ir}$ , and tentatively at 644 keV in  $^{189}\text{Ir}$ .

#### F. $\frac{7}{2}^+$ [404 $\downarrow$ ] orbital

States at 748 and 686 keV in  $^{189}\text{Ir}$  and  $^{191}\text{Ir}$  have been tentatively identified with the  $\frac{7}{2}^+$  [404 $\downarrow$ ] orbital.<sup>4,6</sup> Furthermore this state is expected to be intimately mixed with the  $(K+2)$   $\gamma$  band built on the ground state. The  $\frac{7}{2}^+$  [404 $\downarrow$ ] and  $\frac{3}{2}^+$  [402 $\uparrow$ ] orbitals satisfy the selection rules for coupling by large  $E2$  matrix elements. The strong Coulomb excitation<sup>7</sup> of the 686-keV state in  $^{191}\text{Ir}$  strongly suggests that it is partially a  $(K+2)$   $\gamma$  band built on the ground state.

#### G. $L=0$ angular distributions

The  $L=0$  angular distributions for the reactions  $^{191}\text{Ir}(p, t)$   $^{189}\text{Ir}$  and  $^{193}\text{Ir}(p, t)$   $^{191}\text{Ir}$  are shown in Figs. 3 and 6, respectively. They are the only  $(p, t)$  angular distributions which are distinctive enough to define a unique  $L$  transfer. This can be seen by comparing Fig. 3 with Figs. 4 and 5 and Fig. 6 with Figs. 7 and 8. States populated with an  $L=0$  distribution must have a spin and parity of  $\frac{3}{2}^+$ . It is impressive that a number of strongly populated  $L=0$  distributions are observed for states in the region  $1000 \pm 300$  keV. Indeed the most strongly populated excited state is the  $\frac{3}{2}^+$  state at 1261 keV in  $^{189}\text{Ir}$ . Many of these higher states have no easy explanation in terms of Nilsson configurations. Further there appears to be no evidence for pairing



vibrations or pairing isomers in this mass region. It appears as if the ground states had fragmented into these higher-lying excited states. This tendency toward  $L=0$  fragmentation is clearly greater for the  $^{191}\text{Ir}(p,t)$   $^{189}\text{Ir}$  reaction than for the  $^{193}\text{Ir}(p,t)$   $^{191}\text{Ir}$  reaction. This may imply a greater shape change between  $^{191}\text{Ir}$  and  $^{189}\text{Ir}$  than between  $^{193}\text{Ir}$  and  $^{191}\text{Ir}$ , in much the same way that there is a greater  $L=0$  population of excited states in the reaction  $^{150}\text{Sm}(t,p)$   $^{152}\text{Sm}$  than in the reaction  $^{148}\text{Sm}(t,p)$   $^{150}\text{Sm}$ . In the Sm transition region, there is a large  $L=0$  population of excited states as well as the ground state. This suggests considerable softness in the potential energy as a function of shape for both the target and residual nuclei. This allows considerable overlap in the target wave function and a variety of different nuclear shapes in the residual nuclei. A similar explanation may apply in the Ir transition region, except that here one has in addition a single  $\frac{3}{2}^+$  spectator proton. The effect is, however, not nearly as dramatic for Ir as for Sm. It is in fact interesting that one of the strong  $L=0$  transitions populating a level in  $^{189}\text{Ir}$  at 916.5 keV is exceptionally close to the excited  $0^+$  state in  $^{190}\text{Pt}$  at 921 keV.

Perhaps the single most interesting feature observed in both  $^{189}\text{Ir}$  and  $^{191}\text{Ir}$  is that the angular distributions of the known  $\frac{3}{2}^+$  members of the  $\frac{1}{2}^+[400\uparrow]$  bands are very different from the  $L=0$  angular distributions of all other known  $\frac{3}{2}^+$  states. This is shown in Figs. 3 and 6 where the angular distributions of the  $\frac{3}{2}^+$  members of the  $\frac{1}{2}^+[400\uparrow]$  bands are seen to be very similar to each other but very different from the  $\frac{3}{2}^+$  ground states. Why this should be so is not well understood. However, since the  $\frac{3}{2}^+$  member of the  $\frac{1}{2}^+[400\uparrow]$  band in  $^{191}\text{Ir}$  is strongly populated in inelastic deuteron scattering, it may be significantly populated by second-order processes in the  $(p,t)$  reaction. In such a case, the angular distribution would not then resemble that of a one-step  $L=0$  transition.

#### H. Population of the $\frac{1}{2}^-$ state in $^{189}\text{Ir}$

The  $\frac{1}{2}^-$  state at 371.9 keV in  $^{189}\text{Ir}$  has been described<sup>9</sup> as a hole in the  $^{190}\text{Pt}$  core, with a much smaller deformation than the ground state. It has also been described<sup>6,8</sup> in terms of an asymmetric shape, which could explain the unusual "band" sequence  $\frac{1}{2}^-, \frac{7}{2}^-, \frac{13}{2}^-, \frac{15}{2}^-, \frac{9}{2}^-, \dots$  and the large  $B(E2)$  connecting the  $\frac{7}{2}^-$  and  $\frac{1}{2}^-$  states. It is extremely interesting that the  $(p,t)$  reaction populates this state in  $^{189}\text{Ir}$  although very weakly. This seems to suggest that both the  $^{191}\text{Ir}$  target and the  $^{189}\text{Ir}$   $\frac{1}{2}^-$

potential surfaces are soft enough to allow sufficient overlap in the wave functions to overcome the shape forbiddenness, or that the shapes are not as different as previously envisioned (see conclusion).

#### V. CONCLUSION

The  $(p,t)$  reaction populates a number of low-lying positive-parity states in  $^{189}\text{Ir}$  and  $^{191}\text{Ir}$  which are related to the target ground states. It should be pointed out that although it is possible to interpret these low-lying positive-parity states as members of the  $\frac{3}{2}^+[402\uparrow]$  and  $\frac{1}{2}^+[400\uparrow]$  bands Coriolis coupled and  $(K-2)$   $\gamma$  vibrationally coupled to each other, another interpretation is also possible. In this alternative interpretation, the ground-state nuclear shapes are assumed to be triaxial. The  $\frac{3}{2}^+$  bands will then have associated with them additional states with  $J^\pi = \frac{1}{2}^+, \frac{3}{2}^+, \frac{5}{2}^+$ , etc. In this connection it is interesting to note that the isobars  $^{189}\text{Os}$  and  $^{191}\text{Os}$  have both been shown<sup>12,13</sup> to have triaxial configurations. Such an interpretation could help to explain the population of the  $\frac{1}{2}^-$  band which has also been interpreted as triaxial.

Unfortunately, calculations for reaction cross sections are presently unavailable for triaxial nuclei. It would be very interesting to see if the anomalous angular distributions of the  $\frac{3}{2}^+$  states could be explained assuming triaxiality for both target and residual nuclei, and whether or not it is possible to distinguish between the different proposed shapes using the differential cross sections.

The nature of the higher  $\frac{3}{2}^+$  states with  $L=0$  distributions in  $^{189}\text{Ir}$  represents a challenge to both the experimentalist and the theorist. Experimentally, it would be very valuable to observe the rotational bands associated with these states if indeed such bands exist. Theoretically, it is important to understand the nature of the fragmentation of  $L=0$  strength and to understand the magnitude of the change going from  $^{191}\text{Ir}(t,p)$   $^{189}\text{Ir}$  to  $^{193}\text{Ir}(t,p)$   $^{191}\text{Ir}$ .

In summary, the present study has identified a number of new states and some new problems, thereby demonstrating again the richness of the spectroscopy of the transitional nuclei.

We are grateful to Robert Leonard at Florida State University for preparation of the targets. This work was performed under the auspices of the U. S. Department of Energy, including contract No. W-7405-Eng-48, and the National Science Foundation.

†Current address: Department of Physics, Technical University of Munich, Garching, West Germany.

<sup>1</sup>K. Kumar and M. Baranger, Nucl. Phys. A122, 273 (1968).

<sup>2</sup>U. Gotz, H. C. Pauli, K. Alder, and K. Junker, Nucl. Phys. A192, 1 (1972).

<sup>3</sup>R. J. Pryor and J. X. Saladin, Phys. Rev. C 1, 1573 (1970).

<sup>4</sup>G. Hedin and A. Backlin, Nucl. Phys. A184, 214 (1972), and references cited therein.

<sup>5</sup>R. H. Price and M. W. Johns, Nucl. Phys. A174, 497 (1971).

<sup>6</sup>R. H. Price, D. G. Burke, and N. W. Johns, Nucl. Phys. A176, 338 (1971).

<sup>7</sup>P. Nøgaard, K. M. Bisgaard, K. Gregersen, and

P. Morgen, Nucl. Phys. A162, 449 (1971).

<sup>8</sup>S. Andre, J. Boutet, and J. Rivier, J. Treherne, J. Jastrebski, J. Lukasiak, Z. Sujkowshi, and C. Se-bille-Schuck, Nucl. Phys. A243, 229 (1975).

<sup>9</sup>P. Kemnitz, L. Funke, H. Sodan, E. Will, and G. Winter, Nucl. Phys. A245, 221 (1975).

<sup>10</sup>K. Krien, I. C. Oelrich, R. M. DelVecchio, and R. A. Naumann, Phys. Rev. C 15, 1288 (1977).

<sup>11</sup>A. Backlin, V. Berg, and S. G. Malmkog, Nucl. Phys. A156, 647 (1970).

<sup>12</sup>D. Benson, Jr., P. Kleinheinz, R. K. Sheline, and E. B. Shera, Phys. Rev. C 14, 2095 (1976).

<sup>13</sup>D. Benson, Jr., P. Kleinheinz, R. K. Sheline, and E. B. Shera, Z. Phys. A281, 145 (1977).